Journal of
Measurement, Control and Automation
Đo lường, Điều khiển và Tự động hóa

MỤC LỤC

CONTENTS

An improvement of the miniaturized microstrip patch antenna based on coupled microstrips for on-body sensors

Thi Lan Tran*, Thi Xuan Dang, Quang Khai Trinh, Van Lam Phi

University of Transport and Communications
Faculty of Electrical and Electronic Engineering
*Corresponding author E-mail:ttlan@utc.edu.vn

Abstract

This paper presents a low-cost miniaturized microstrip patch antenna (MPA) designed for on-body applications at a frequency of 2.45 GHz. The antenna is based on the coupled-microstrip principle using FR-4 material. The microstrip transmission line feeding method is used to easily integrate the antenna into the sensor chip on the same plane. The antenna has a gain of 2.28 dBi, a bandwidth of 2.62%, an efficiency of 46.5%, and overall dimensions of 48.6×48.6×1.6 mm³. To evaluate the performance of the proposed antenna, it is compared with three different antenna versions, considering the impact of the human body on the antenna and the specific absorption rate (SAR) of the human body. The proposed antenna shows excellent compliance with the requirements for on-body sensor antennas.

Keywords: *Miniaturized Antenna, Microstrip Antenna, SAR, On-body Sensors, Microstrip Feeding.*

1. Introduction

Sensors that measure biometric parameters on the human body play an increasingly important role in modern life [1-2]. These sensors need to be compact so that patients feel comfortable wearing them on their bodies all the time. Consequently, the antennas inside these sensors also need to be increasingly miniaturized. Microstrip patch antennas (MPAs) are used in various fields such as GPS (Global Positioning System), satellites, reader antennas in ETC (Electronic toll collection) systems, element antennas in base stations, and Wi-Fi [3-8], due to their ease of fabrication and low cost. Therefore, they are also applied to on-body sensors. Some methods for miniaturizing MPAs include utilizing a substrate with a high relative permittivity (εr), slot-cutting in the radiating patch, reshaping the ground plane and antenna, shorting and folding the patch antenna, and the use of metamaterials [3-4]. The length of the patch is inversely proportional to the square root of the relative permittivity (εr). However, using a substrate with high relative permittivity increases surface wave excitation within the substrate, resulting in lower bandwidth and decreased radiation efficiency.

A MPA can also be miniaturized by altering the shape of the patch or adding slots. However, miniaturized MPAs suffer from higher ohmic losses, leading to lower radiation efficiency. While this method is widely used and offers several degrees of miniaturization, it lacks a general design methodology. Most designs based on this method have low radiation efficiency but provide wider operating bandwidths when using slots [11].

MPAs can also be miniaturized by modifying their ground plane, such as inserting various types of slots. Properly designed slots increase the current path within the patch area, lowering the resonant frequency and reducing the size. However, using defected ground structures (DGS) usually results in lower efficiency and narrower operating bandwidths [12]. Additionally, re-tuning the antenna is often needed to compensate for the shift in resonant frequency due to

alterations in ground currents, especially if the DGS is close to resonant structures. This method may also increase the back lobe, leading to a higher Specific Absorption Rate (SAR).

Although metasurfaces have been successful in reducing antenna size, this comes at a substantial cost, including the use of complex materials, very narrow operating bandwidths, low radiation efficiency, and increased antenna thickness.

Combining different antenna miniaturization methods yields better results than using these methods independently. According to [13], combining slot-cutting with metamaterials or shorting pins with metamaterials is proposed to improve antenna performance, although it slightly increases the antenna's thickness.

In [14], a novel method for miniaturizing microstrip patch antennas using coupled microstrip and shorting pins was proposed at 8.45 GHz. The antenna, fed by a coaxial cable, had a single layer, making it challenging to integrate into on-body sensors on the same plane. Additionally, it utilized the Rogers4330 substrate, which is not commonly used for electronic circuits. Therefore, a new version of this antenna using a low-cost FR-4 substrate at 2.45 GHz is proposed to make it more suitable for on-body applications. In the new version, the microstrip feeding method is applied for easier integration into on-body sensors. The body effect on the antenna and the Specific Absorption Rate (SAR) will also be considered. The remainder of this paper presents the design principles of the proposed antenna using the coupled-microstrip method and discusses its performance.

2. Antenna design

1.1. Coupled microstrip antenna

The proposed antenna, as shown in Figure 1(d), uses a low-cost FR-4 substrate instead of Rogers4330 and operates at a frequency of 2.45 GHz, compared to the antenna in [14]. Notably, the antenna is fed by a microstrip transmission line

instead of a coaxial cable, making it easier to integrate with sensor circuits. To evaluate the performance of the proposed antenna against the antenna in [14], the performance of antenna versions V1, V2, and V3, as shown in Figures 1(a), 1(b), and 1(c), respectively, is discussed. The dimension parameters are given in Table 1. The antennas in these versions are smaller than the original V1 antenna.

Table 1: Dimension parameters

Parameters [mm]	Proposed (V0)	V1	V2	V3
w	24.6	28.2	24.8	24.8
w_g	48.6	52.2	48.8	48.6
l_{fc}	11	7	7	
w_f	2.86			2.86
g_1	0.3		0.3	0.3
g_2	0.3			
d	4.5		4.9	4.9
r	0.5		0.5	0.5
l_f	12			12

Table 2: A comparison between versions of the proposed antenna

Parameters @2.45 GHz	Proposed	V1	V2	V3
S11 [dB]	-22.2	-19.2	-29.7	-6.5
Peak gain [dBi]	2.28	2.7	2.52	0.84
BW[%]	2.62	3.1	2.93	0
Efficiency [%]	46.5	44.3	48.1	42
HPBW [degree]	101.5	96.3	101.1	101.7
Back lobe [dB]	-8.7	-11.8	-8.6	-8.7

First, a simple square patch antenna (V1) fed by a coaxial cable is simulated as shown in Figure 1(a). This is the original antenna for comparison in the next sections. The second version (V2) has a structure similar to the antenna in [14], as shown in Figure 1(c). However, the FR-4 substrate is used instead of the Rogers4330 substrate to reduce manufacturing costs and is designed to operate at 2.45 GHz. FR-4 is one of the most low-cost and popular materials used for circuit prototypes, but it is not ideal for antenna fabrication due to its high tangent loss (tanδ = 0.025).

V2 incorporates gaps in the patch to divide it into smaller sections and adds shorting pins at the edges to function as shorting walls. V2 operates in the TM10 mode [14]. Compared to V1, the length W of V2 is reduced to 24.8 mm, and the efficiency increases by approximately 3%. However, the gain and bandwidth (BW) decrease. When g_1 increases, the resonant frequency shifts to a higher band, as shown in Figure 2. The optimal value of g_1 is 0.3 mm for practical fabrication and balancing the size and gain of the antenna. The radius of the pins affects the resonant frequency and gain of the antenna. As the radius increases, the gain improves, but the operating frequency shifts to a higher band, as shown in Figure 3.
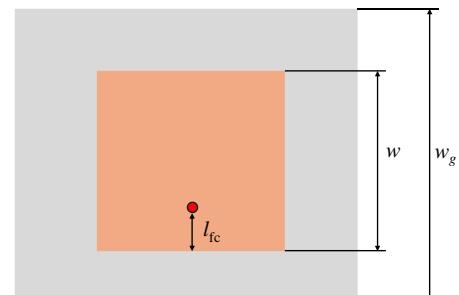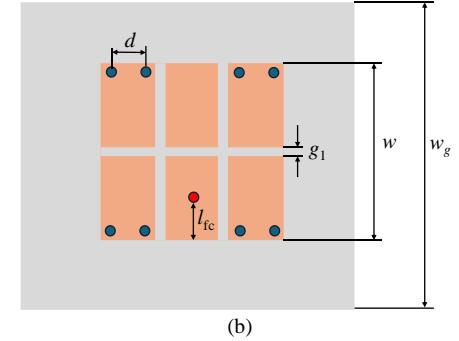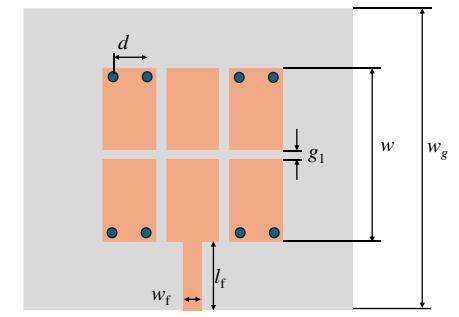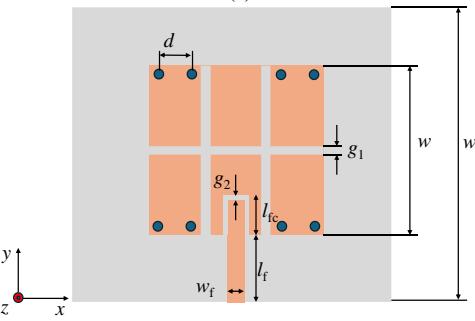

Figure 1: Structure of the proposed antenna: (a) Version 1 (V1), (b) Version 2 (V2), (c) Version 3 (V3), and (d) The proposed antenna.
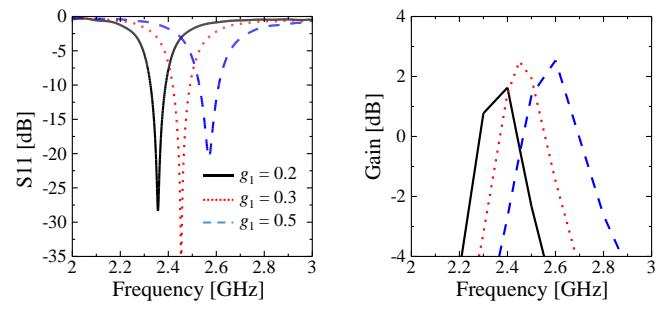

**Figure 2**: Effect of g_1 on the antenna V2: (a) S11, and (b) Gain.

(a)   (b)
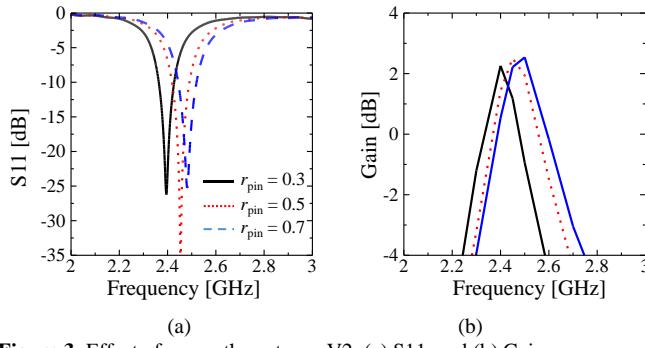
Figure 3: Effect of r_{pin} on the antenna V2: (a) S11, and (b) Gain.

(a)   (b)

(c)
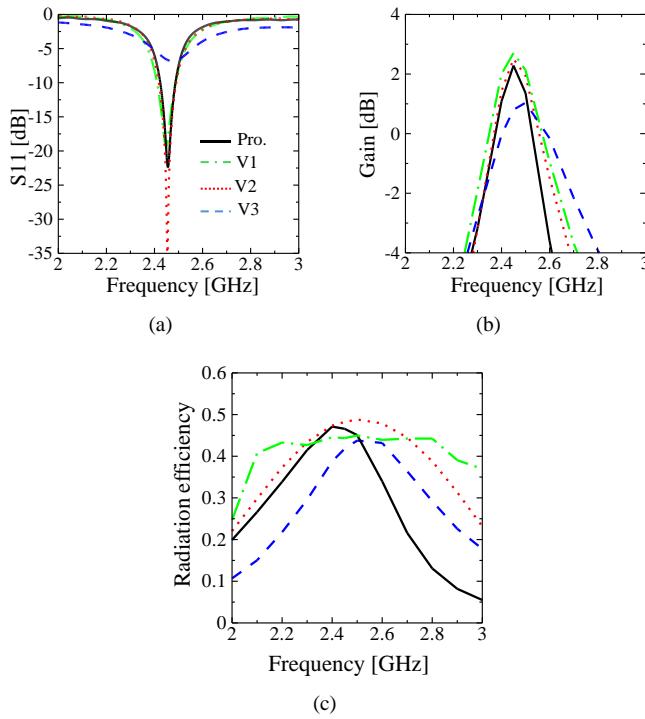
Figure 4: The performance of the antennas V1, V2, and V3 compared to the proposed antenna in (a) S11, (b) gain, and (c) efficiency.
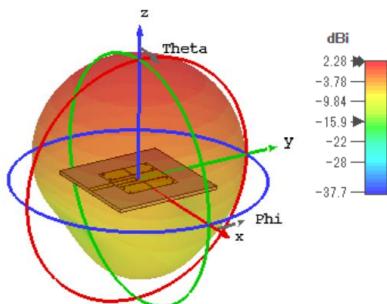

Figure 5: Radiation pattern of the proposed antenna at 2.45 GHz.

To facilitate the integration of the antenna into the on-body sensor circuit on a single plane, the coaxial feeding method is replaced with the microstrip feeding method. The input impedance undergoes significant changes when transitioning from V2 to V3, as illustrated by the dashed blue lines in Figure 4, due to the alteration in the antenna's input impedance. Subsequently, the feeding line is adjusted to match the antenna's impedance, as depicted in Figure 1(d). A U-shaped slot is employed to create a coupling between the feeding microstrip line and the square patch.

Figure 4 shows the simulation results for S11, gain, and efficiency of the four antennas in Figure 1. The size of the radiating part decreases across the antenna versions. However, the bandwidth also decreases. V1 has the largest size and the lowest efficiency at 2.45 GHz, but it has the highest gain and bandwidth. Meanwhile, versions V2, V3, and the proposed antenna have higher efficiency but slightly reduced bandwidth and gain. Detailed comparisons between the versions are presented in Table 2. Figure 5 shows the radiation pattern of the proposed antenna in free space, with a peak gain of 2.28 dBi.

1.2. Body effect

The body effect can influence various aspects of an antenna's operation, including its radiation pattern, impedance, efficiency, and resonant frequency. This effect is especially relevant in wearable and mobile devices, such as smartphones, body-worn sensors, and other wireless communication systems, where antennas are close to the human body [15-17].

To evaluate the impact of the human body on the performance of the proposed antenna, this section conducts simulations to assess the antenna's performance when placed on a simplified human body model [18], as shown in Figure 6. The detailed electrical parameters of the body model tissues are provided in Table 3 [19].

By varying the distance h between the antenna and the human body model from 1 mm to 10 mm, changes in S11, gain are analyzed. From the simulation results in Figure 7(a), it can be observed that when the antenna is close to the human body, the resonant frequency shifts to a lower frequency. This shift is less pronounced as the antenna is placed further from the body. To compensate for the frequency shift, the antenna should have a wide bandwidth. In this study, the width W is adjusted from 24.6 mm to 23.35 mm in the case of $h = 1$ mm, as shown in Figure 8.

The antenna gain increases as h increases, as shown in Figure 7(b). Especially, the gain reduces significantly compared to it in free space. This is because the human body absorbs more electromagnetic waves when the antenna is closer to the body. Therefore, on-body antennas should be placed as far from the body as possible to avoid energy absorption by the body.
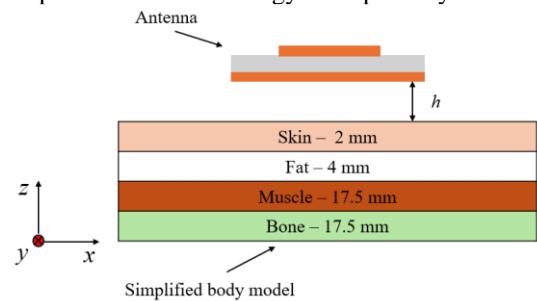
Figure 6: The proposed antenna on the body simplified model.

Table 3: Dielectric properties of tissues

| Tissue	Permittivity (ε)	Conductivity (σ) [S/m]	Loss Tangent (tan δ)	Mass density [g/cm³]
Skin	38-42	1.46	0.18	1.1
Fat	5.69	0.03	0.005	0.92
Muscle	52.7	1.73	0.33	1.06
Bone	12.45	0.14	0.01	1.85

(a)   (b)
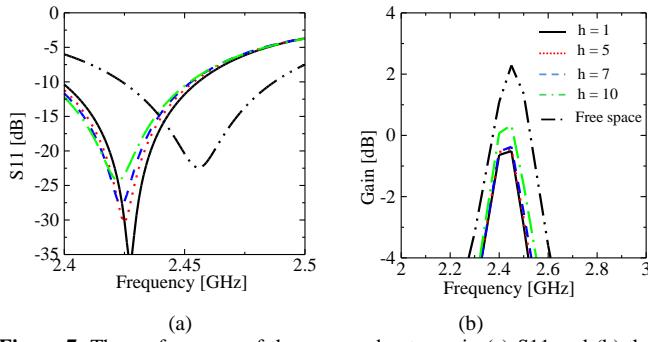
**Figure 7**: The performance of the proposed antenna in (a) S11 and (b) the gain of the antenna on the simplified body model.
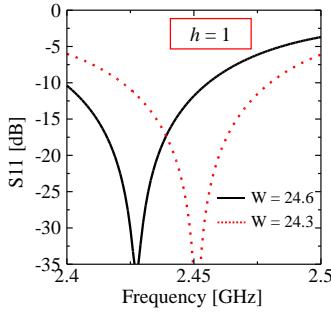
Figure 8: Simulated S11 of the proposed antenna on the simplified body model after W is adjusted shorter with h = 1 mm.

1.3. SAR calculation

Specific Absorption Rate (SAR) is a measure of the rate at which energy is absorbed by the human body when exposed to an electromagnetic field. It is typically expressed in watts per kilogram (W/kg) and is used to ensure that devices are safe for human use. SAR values are determined by the power density of the electromagnetic field ($|E|^2$) and the properties of the tissue absorbing the energy [20-21] as shown in Equation (1).

$$SAR = \frac{\sigma |E|^2}{\rho} \tag{1}$$

Where σ and ρ represent the electric conductivity (S/m) and mass density (kg/m3) of the medium, respectively. The limits on SAR levels to protect public health are given in Table 4 [21].

In this section, we perform SAR calculations using CST Studio Suite 2019 software [22] with the assumption that the sensor power is around several milliwatts (mW), which is a common power level for sensors on the human body [23]. In this simulation case, we consider h = 1mm, and the transmitting power is 0 dBm. The maximum SAR result shown in Figure 9 is 0.000546 W/kg with an average mass of 10 g. This result satisfies both standards in Table 4.

Table 4: SAR limits for public health

| Standard	SAR limit [W/Kg]	Averaging mass for SAR
ICNIRP	2.0 (f < 10 GHz)	10 g of tissues
FCC/ANSI	1.6 (f < 6 GHz)	10 g of tissues
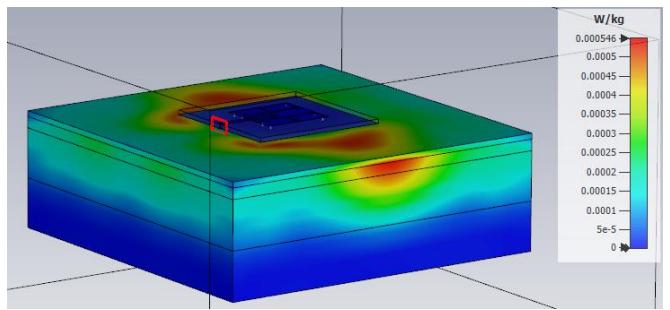
Figure 9: Simulation result of the maximum SAR over 10 g at 2.45 GHz.

3.   Conclusion

This paper presented an improvement of the antenna in [14]. The proposed antenna is easily integrated into on-body sensors thanks to microstrip line feeding combined with the coupling method. The size of the proposed antenna is significantly reduced while the gain and the efficiency remain. This result will be the basis for research on miniaturizing antennas for body-worn sensors. Additionally, the effect of the human body is evaluated by simulating the antenna on a simplified body model. The results show that the closer to the body, the more electromagnetic wave energy is absorbed, and the resonant frequency shifts to a lower frequency. This result can be used for future research to mitigate the impact on the human body. The proposed antenna has a SAR index that meets health safety standards. In the future, the proposed antenna will be optimized, fabricated, and measured.

Acknowledgment

References

[1]   Mukhopadhyay, S. C., Suryadevara, N. K., & Nag, A. (2022). Wearable Sensors for Healthcare: Fabrication to Application. Sensors, 22(14), 5137. https://doi.org/10.3390/s22145137

[2]   D. M. G. Preethichandra, L. Piyathilaka, U. Izhar, R. Samarasinghe and L. C. De Silva, "Wireless Body Area Networks and Their Applications—A Review," in IEEE Access, vol. 11, pp. 9202-9220, 2023, https://doi.org/10.1109/ACCESS.2023.3239008.

[3]   [3] K. D. Chinh and T. T. Lan. (2021). A Circularly Polarized Array Antenna for GPS Application, NAFOSTED Conference on Information and Computer Science (NICS), Hanoi, Vietnam, 2021, pp. 29-32, https://doi.org/10.1109/NICS54270.2021.9701530

[4]   [4] Apriono, C., Mahatmanto, B. P. A., & Juwono, F. H. (2023). Rectangular Microstrip Array Feed Antenna for C-Band Satellite Communications: Preliminary Results. Remote Sensing, 15(4), 1126. https://doi.org/10.3390/rs15041126

[5]   [5] L. T. . Tran, C. D. . Khuat, and L. V. . Phi. (2023). A Wideband, High Gain and Low Sidelobe Array Antenna for Modern ETC Systems", ACES Journal, vol. 38, no. 05, pp. 333–342.

[6]   [6] F. -C. Chen, Y. -Z. Liang, W. -F. Zeng and K. -R. Xiang. (2024). A Series-Fed Slant-Polarized Microstrip Patch Antenna Array. IEEE Transactions on Antennas and Propagation, vol. 72, no. 6, pp. 5367-5372, https://doi.org/10.1109/TAP.2024.3394215.

[7]   [7] N. -S. Nie, X. -S. Yang, Z. N. Chen and B. -Z. Wang. (2020). A Low-Profile Wideband Hybrid Metasurface Antenna Array for 5G and WiFi Systems. IEEE Transactions on Antennas and Propagation, vol. 68, no. 2, pp. 665-671, https://doi.org/10.1109/TAP.2019.2940367.

[8] [8] Praveen Kumar Malik, Sanjeevi kumar Padmanaban and Jens Bo Holm-Nielsen. (2022). Microstrip Antenna Design for Wireless Applications. CRC Press. https://doi.org/10.1201/9781003093558.

[9] Muhammad Umar Khan, Mohammad Said Sharawi, Raj Mittra. (2015). Microstrip patch antenna miniaturisation techniques: a review. IET Microwaves, Antennas & Propagation, Volume 9, Issue 9 p. 913-922. https://doi.org/10.1049/iet-map.2014.0602

[10] K. N. Paracha, S. K. Abdul Rahim, P. J. Soh and M. Khalily, "Wearable Antennas: A Review of Materials, Structures, and Innovative Features for Autonomous Communication and Sensing," in IEEE Access, vol. 7, pp. 56694-56712, 2019, https://doi.org/10.1109/ACCESS.2019.2909146.

[11] Hung Tien Nguyen, S. Noghanian and L. Shafai. (2005). Microstrip patch miniaturization by slots loading. IEEE Antennas and Propagation Society International Symposium, Washington, DC, USA, pp. 215-218 vol. 1B, https://doi.org/10.1109/APS.2005.1551525.

[12] Sarkar, S., Majumdar, A.D., Mondal, S., Biswas, S., Sarkar, D., Sarkar, P.P. (2011). Miniaturization of rectangular microstrip patch antenna using optimized single-slotted ground plane. Microw. Opt. Technol. Lett., 53, (1), pp. 111–115. https://doi.org/10.1002/mop.25661

[13] Lan Thi Tran, Lam Van Phi. (2024). Analyzing Microstrip Antenna Miniaturization Methods for Wearable IoT Sensors, *IEEE International Conferences On Antenna Measurements and Applications,* Vietnam.

[14] Z. Shao and Y. Zhang, "A Single-Layer Miniaturized Patch Antenna Based on Coupled Microstrips," in IEEE Antennas and Wireless Propagation Letters, vol. 20, no. 5, pp. 823-827, May 2021, https://doi.org/10.1109/LAWP.2021.3064908.

[15] Casula, G. A., & Montisci, G. (2019). A Design Rule to Reduce the Human Body Effect on Wearable PIFA Antennas. Electronics, 8(2), 244. https://doi.org/10.3390/electronics8020244

[16] T. T. Lan, Y. Shinozaki, T. Okura and H. Arai. (2018). A Free-Access Segmented Coplanar Waveguide for On-Body Communication," in IEEE Transactions on Antennas and Propagation, vol. 66, no. 9, pp. 4524-4532, https://doi.org/10.1109/TAP.2018.2842302.

[17] T. T. Lan, Y. Shinozaki and H. Arai. (2017). A flexible transmission line using a coplanar waveguide for on-body links. International Symposium on Antennas and Propagation (ISAP), Phuket, Thailand, pp. 1-2, https://doi.org/10.1109/ISANP.2017.8228889.

[18] M. Rizwan, M. W. A. Khan, L. Sydänheimo and L. Ukkonen, "Performance evaluation of circularly polarized patch antenna on flexible EPDM substrate near human body," *2015 Loughborough Antennas & Propagation Conference (LAPC)*, Loughborough, UK, 2015, pp. 1-5, https://doi.org/10.1109/LAPC.2015.7366118.

[19] Tissue Properties. Available: https://itis.swiss/virtual-population/tissue-properties/database/dielectric-properties/

[20] T. T. Lan and H. Arai, "Propagation Loss Reduction Between On-Body Antennas by Using a Conductive Strip Line," in *IEEE Antennas and Wireless Propagation Letters*, vol. 17, no. 12, pp. 2449-2453, Dec. 2018, https://doi.org/10.1109/LAWP.2018.2877772.

[21] Tooba Hamed and Moazam Maqsood. (2018). SAR Calculation & Temperature Response of Human Body Exposure to Electromagnetic Radiations at 28, 40 and 60 GHz mmWave Frequencies. Progress In Electromagnetics Research M, Vol. 73, 47–59.

[22] CST studio suite. Available: https://www.3ds.com/products/simulia/cst-studio-suite

[23] Rong, Guoguang, Yuqiao Zheng, and Mohamad Sawan. (2021). Energy Solutions for Wearable Sensors: A Review. Sensors 21, no. 11: 3806. https://doi.org/10.3390/s21113806.

Home / Announcements /

The journal Measurement, Control and Automation will be recognized at a level of 0-1.0 points from 2024.

The journal Measurement, Control and Automation will be recognized at a level of 0-1.0 points from 2024.

📅 11-07-2024

The State Council of Professors (HĐGSNN) recently issued Decision No. 25/QD-HDGSNN issued on July 5, 2024 approving the list of scientific journals to be scored in 2024. Accordingly, the Specialized Journal of Measurement and Control The Vietnam Automation Association's Control and Automation score will be increased from 0-0.75 to 0-1.0 points from 2024.

Make a Submission

Browse

Language

English

Tiếng Việt

Information

For Readers

For Authors

For Librarians

Current Issue

ATOM 1.0

RSS 2.0